

# PROBABILISTIC PERFORMANCE ASSESSMENT OF LOW-DUCTILITY RC FRAMES RETROFITTED WITH DISSIPATIVE BRACES

## **Fabio FREDDI**

Title Ph.D.

## **Laura RAGNI**

Title Assistant Professor

University or Affiliation Marche Polytechnic University

Address Via Breccie Bianche,60131 Ancona, Italy

email address\* *f.freddi@univpm.it, laura.ragni@univpm.it*

## **Enrico TUBALDI**

Title Ph.D.

## **Andrea DALL'ASTA**

Title Full Professor

University or Affiliation University of Camerino

Address Viale Rimembranza, 63100 Ascoli Piceno, Italy

email address *etubaldi@libero.it, andrea.dallasta@unicam.it*

## **Abstract**

The paper illustrates a probabilistic methodology for assessing the vulnerability of existing reinforced concrete (RC) buildings with limited ductility capacity retrofitted by dissipative braces. The aim is to highlight the most important parameters controlling the capacity of these coupled systems and specific aspects concerning the response uncertainties. The proposed methodology is based on the development of fragility curves by performing incremental dynamic analysis within OpenSees and on the use of local engineering demand parameters. The capabilities of the methodology are tested by considering a benchmark RC frame designed for gravity-loads only and retrofitted by introducing elasto-plastic dissipative braces. The results show the effectiveness of the methodology and of the employed simulation software in describing the change of failure modalities due to retrofit.

**Keywords:** Reinforced concrete frames, seismic vulnerability, fragility curves, seismic retrofit, buckling-restrained braces, probabilistic methodology.

## **1. Introduction**

The damage occurred during recent earthquakes in many existing reinforced concrete (RC) buildings designed before the introduction of modern seismic codes has shown that these structures are very vulnerable to the seismic action due to their reduced ductility capacity. Thus, there is a significant need of modern retrofit techniques for increasing their safety and of reliable tools for assessing the effectiveness of the retrofit.

Among the various techniques currently employed for the retrofit, the use of dissipative braces appears to be very promising [1]. These braces provide a supplemental path for the earthquake induced horizontal actions and thus enhance the seismic behavior of the frame by adding dissipation capacity and, in some cases, stiffness to the bare frame. However, the introduction of a bracing system into a frame often induces remarkable changes in the collapse modalities and in the probabilistic properties of the seismic response of the structure. Therefore, the effectiveness of this retrofit technique should be evaluated within a probabilistic framework. A popular approach for assessing in the seismic vulnerability of structural systems involves the development of fragility curves. These tools provide the probability of exceeding a specified limit state (LS), conditional to the ground motion (g.m.)

shaking severity, quantified by an appropriate intensity measure ( $IM$ ). For example, fragility curves are employed by [2] investigating the effectiveness of several retrofit techniques, such as addition of shear walls and column jacketing, but only few works ([3],[4]) analyze the impact of the use of bracing system. These studies employ global engineering demand parameters (EDPs) such as the peak interstory drift for monitoring the seismic response of the frame and of the retrofit system. Although this strategy is convenient from a computational point of view, it may be inappropriate for the particular case analyzed. In fact, global EDPs are able to capture the local failure only if the structural elements are adequately proportioned. This is the case of ductile structures designed by following modern seismic rules such as strength hierarchy (capacity design) and provided with proper seismic detailing. These conditions are not respected in many existing frames. By contrast, monitoring local component EDPs [5], such as the strain demand at the critical element sections or the shear demand on a beam-column joints, permits to control the probabilistic response of single resisting components. This allows to assess their contribution to the system vulnerability and the impact of the retrofit on the local response of the individual members. For this purpose the Finite Element (FE) model used for simulating the structural response should be such that: 1) local EDP can be monitored, 2) local behavior of frame components and of the retrofit system can be reproduced with accuracy, 3) results of simulation can be easily managed and post-processed, 4) numerous analyses are rapidly performed. The OpenSees framework satisfies all of these requirements and thus is used in this study. The present study illustrate how the OpenSees framework [9] can address all these needs by considering the vulnerability assessment of a low-ductility RC frame retrofitted by elasto-plastic dissipative braces.

## 2. Probabilistic methodology for Vulnerability Assessment

The probabilistic seismic response assessment should consider several sources of uncertainties. In this case, the earthquake input randomness is taken into account by selecting a set of natural g.m. records while the model parameters and epistemic uncertainty are disregarded. In order to generate fragility curves, incremental dynamic analysis (IDA) [6] is performed by subjecting the system to a set of g.m. records for increasing values of the  $IM$  assumed as the spectral acceleration  $S_a(T)$  at the fundamental period of the structure  $T$  for a damping factor  $\zeta=5\%$ . IDA provides a set of demand samples of appropriately selected EDPs monitoring the system response for discrete  $IM$  values. As already discussed in the introduction, local EDPs, directly related to the component failure modes, are used in order to monitor the behavior of the components and to capture the modifications of the frame response and of the collapse modalities induced by the introduction of the bracing system. The seismic demand on the frame elements related to flexural moments and axial forces is controlled by monitoring the maximum-over-time values of the concrete compressive strain  $\varepsilon_c$  and of the steel strain  $\varepsilon_s$  at the most critical sections. The non-ductile mechanisms are controlled by recording the maximum-over-time values of the shear force  $V$  at the critical sections of each element, the diagonal tension stress  $\sigma_t$ , and the diagonal compression stress  $\sigma_c$  at each beam-column joint. Finally, in the retrofitted case, the seismic demand on the retrofit system is controlled by the maximum-over-time value of the ductility demand  $\mu_d$  for each dissipative brace. Component fragility curves are built for the LSs reported in Tab. 1.

Component fragilities are defined by the comparison of the samples of the demand with the corresponding capacity, while, system fragility curves are derived by assuming a series arrangement of the components. The series arrangement assumption made is consistent with the seismic code prescriptions requiring that all the considered LSs must be verified for all the structural members. The numerical fragility curves are fitted by analytical lognormal curves obtained through least-square minimization. This methodology permits to draw some important considerations regarding the performance of the system before and after the retrofit.

In fact, by directly comparing the single component fragility curves to each other and to the system fragility curve, it is possible to evaluate the most vulnerable components and their contribution to the system vulnerability.

**Table 1. Limit states**

EDPs	Capacity limits	LSs
$\varepsilon_c$	$\varepsilon_{cu}$	LS1: concrete failure of frame elements
$\varepsilon_s$	$\varepsilon_{su}$	LS2: steel failure of frame elements
$V$	$V_u$	LS3: shear failure of frame elements
$\sigma_c$	$\sigma_{cu}$	LS4: compression failure of frame joints
$\sigma_t$	$\sigma_{tu}$	LS5: tension failure of frame joints
$\mu_d$	$\mu_{du}$	LS6: failure of dissipative braces

### 3. Case Study

A three story ordinary RC moment resisting frame, is considered to apply the proposed methodology and demonstrate its capability. This case study has been chosen since an extended experimental campaign has been carried out on 1:3 reduced scale models of the frame and of its subassemblages [7][8]. Thus, the detailed information available for the global frame's [8] and the local members' behavior [7] permits an accurate validation of the finite element (FE) model at global and at local scale. Fig. 1 shows the general layout of the structure (complete detailing may be found in [8]).

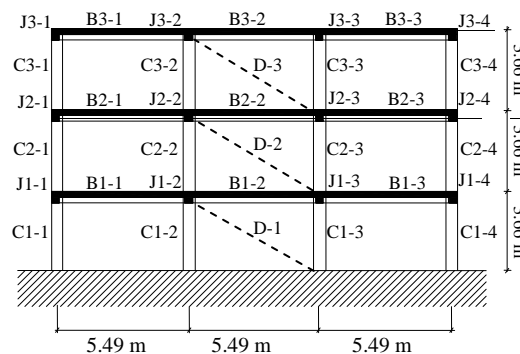


**Figure 1. General layout of the structure and braces arrangement (adapted from [8]).**

The building has been designed for gravity loads only without any seismic detailing, by applying the design rules existing before the introduction of modern seismic codes. The frame consists of three stories 3.66 m high, and of three bays (5.49 m wide). Columns have a 300×300 mm<sup>2</sup> square section while beams are 230×460 mm<sup>2</sup> at each floor. Grade 40 steel ( $f_y = 276$  MPa) and concrete with compression resistance  $f_c' = 24$  MPa were employed in the design. No lateral load has been considered for the design.

A two dimensional FE model of the structure is developed in OpenSees [9]. The “beam with hinges” element [10] is employed to describe the nonlinear hysteretic response of beams and columns. In the plastic hinge zone, the behavior of concrete is described by the non linear degrading Concrete02 material model [9] while the behavior of steel reinforcements is described by the Hysteretic material model [9], whose parameters controlling pinching, damage and degraded unloading stiffness are calibrated to obtain the best fit between the numerical and the experimental results. The plastic hinge length of the elements is evaluated by the formula proposed in [11]. In order to account for concrete cracking, the elastic part of each element is modeled with an effective flexural stiffness, evaluated by means of moment-curvature analysis, for the axial force level induced by the dead loads. The FE model is validated by comparing the experimental results with the simulated test results of the 1:3 scale numerical FE models of the frame and of its subassemblages. The material properties in the scaled models are defined coherently with the results of the experimental test performed on

the materials specimens. In [7], the authors report the results concerning four 1:3 scale column specimens with and without lap splices loaded with low and high levels of axial forces, representing respectively the interior and exterior column at floor slab and at beam soffit levels. The study also reports the results of the tests performed on two 1:3 scale specimens of an exterior and an interior beam-column joint subassemblage. Both the columns and the joints were subjected to reverse cyclic loading for increasing drift amplitudes up to failure. Fig. 2 and 3 show the comparisons between the experimental and the numerical results. The simulated test results show a satisfactory agreement with the experimental results and demonstrate the capability of the FE model to simulate the cyclic local member behavior.

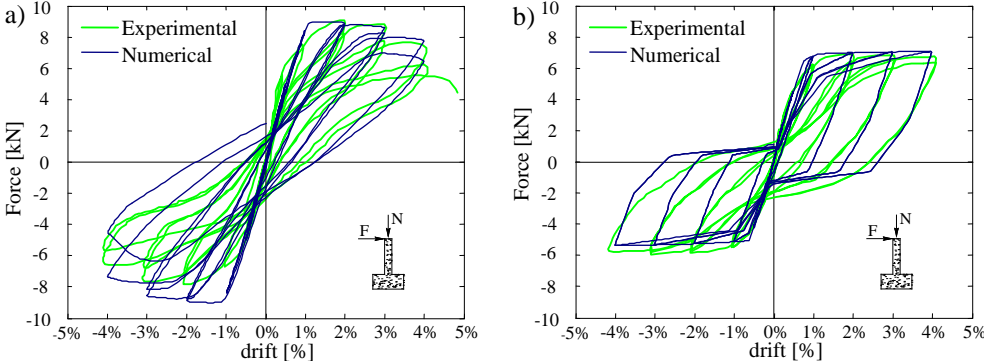


**Figure 2. Experimental and numerical lateral load-drift comparison for column specimen a) with lap splices and high axial load and b) without lap splices and low axial load.**

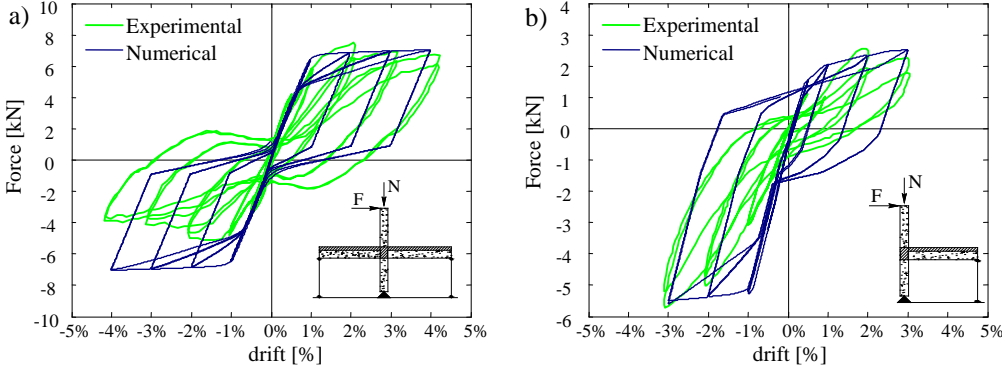


**Figure 3. Experimental and numerical lateral load-drift comparison for interior slab-beam-column subassemblage at a) interior node, and b) exterior node.**

In [8], the results of the experimental tests carried on the 1:3 scale frame are reported. The first three natural periods measured in the experimental test results (0.538, 0.177 and 0.119 sec) are in close agreement with the periods provided by the 1:3 scale FE model with uncracked gross stiffness properties (0.561, 0.180, and 0.110 sec). A good agreement is also observed in the first three modal shapes. Shaking table tests results are also available, describing the time-history of the frame response under the Kern County 1952, Taft Lincoln School Station, N021E component record scaled for different levels of the seismic intensity (PGA = 0.05g, 0.20g and 0.30g). Fig. 4 shows the comparison between the top story displacements of the 1:3 scale experimental and numerical models for the various levels of the seismic intensity. In the FE model, damping sources other than the hysteretic dissipation of energy are modeled through the Rayleigh damping matrix. The values of the mass-related and stiffness-related damping coefficients are such that the best fit to the numerical results is achieved and yield a damping factor of 3% for the first two vibration modes. The agreement between the simulated and experimental response history is very satisfactory for values of the PGA equal to 0.05g and 0.02g, while for PGA = 0.03g the agreement is not as good, although the peak response values are simulated with good accuracy.

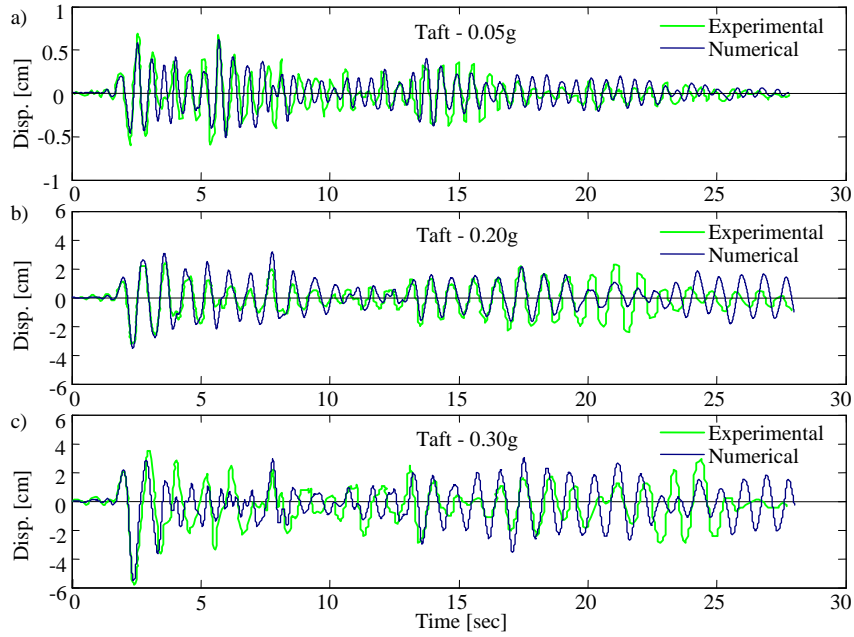


Figure 4. Comparison of numerical and experimental shaking table tests results: top story displacement for a) PGA = 0.05g, b) PGA = 0.20g, and c) PGA = 0.30g.

#### 4. Retrofitting of RC frame with elasto-plastic braces

The BRBs are designed by applying a widespread method based on an equivalent nonlinear SDOF approximation. The interested reader is referred to [12] for a detailed description. Fig. 5a shows the pushover curve obtained for the load distribution relative to the first vibration mode of the bare frame (mass participation factor of 86.4%). The ultimate capacity of the frame members is evaluated by considering the strain demand in the most critical concrete and steel fibers ( $\varepsilon_c$  and  $\varepsilon_s$ ) and the corresponding limits  $\varepsilon_{cu} = 0.0035$  and  $\varepsilon_{su} = 0.04$ . The top story displacement  $d = 0.102$  m denoting the failure of the most critical element (C1-2) is posed in evidence in Fig. 5a and it is assumed as design displacement  $d_u$  for the BRBs. The yielded and failed sections at this displacement value are reported in Fig. 5b. Obviously, after this first failure, the bare frame still possesses a residual capacity and can be pushed up to a top story displacement  $d = 0.183$  m, at which all the base story columns fail (Fig. 5c). Differently from the BRBs commonly used in steel-structures, the dissipative devices employed in this study are quite short in order to obtain low yield displacements and thus, the dissipative diagonal brace is made by assembling the BRB in series with an elastic brace characterized by an adequate over-strength. The BRBs are characterized by an elasto-plastic behavior and in this study are modeled by the Steel 02 [9] material model. The bare frame is retrofitted by inserting a bracing system designed for several retrofit levels, measured by the ratio  $\alpha$  between the base shear capacity of the bracing system  $V_d^l$  and that of the bare frame  $V_f^l$ . Parameter  $\alpha$  range from 0 to 3.2. In Fig. 5a, the pushover curves of the retrofitted frames are reported while, in Tab. 2, the axial yield force  $F_d^i$  and the elastic stiffness  $K_d^i$  of the dissipative braces and the fundamental vibration periods are given for three retrofit levels.

Table 2. Dissipative braces properties at each story

Story	$\alpha=0.4$ ( $T=0.670$ sec)		$\alpha=1.6$ ( $T=0.404$ sec)		$\alpha=3.2$ ( $T=0.321$ sec)	
	$F_d^i$ [kN]	$K_d^i$ [kN/m]	$F_d^i$ [kN]	$K_d^i$ [kN/m]	$F_d^i$ [kN]	$K_d^i$ [kN/m]
1	88	36046	351	144183	702	288365
2	75	25106	301	100423	601	200847
3	43	22921	173	91685	346	183371

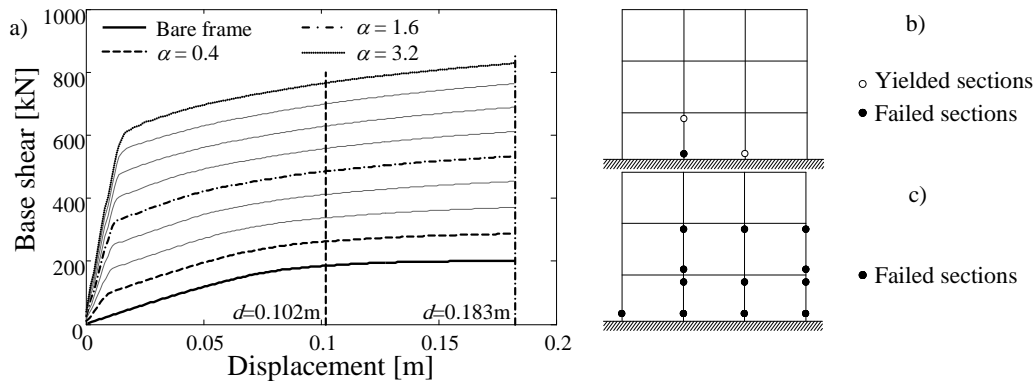


Figure 5. a) Pushover curves for bare and retrofitted frame, b) mapping of plastic hinges at  $d=0.102\text{m}$ , and c) mapping of plastic hinges at  $d=0.183\text{m}$ .

## 5. Vulnerability Assessment

For the purpose of performing IDA, a number of 30 natural g.m. records are selected from the European database. These records are chosen in a range of magnitude and source to site distance of 5.5-7.0 and 25-75 km respectively and are compatible with the type 1 uniform hazard spectrum of Eurocode 8 and with soil type D. For each record, for each  $IM$  value and for each element of the frame, the maximum-over-time values of the EDPs listed in Section 2 have been recorded. The capacity of the tension ( $\sigma_{tu}$ ) and compression ( $\sigma_{cu}$ ) stresses at each joints and the element shear resistance  $V_u$  have been calculated by the formulations proposed in [5]. Coherently with the capacity assumed in the retrofit design procedure, the concrete and steel capacity are set equal to  $\varepsilon_{cu} = 0.0035$  and  $\varepsilon_{su} = 0.04$ . Fig. 6 and 7 report some results of the IDA respectively for the bare and for a retrofitted frame ( $\alpha=1.6$ ).

The component fragility curves are evaluated for each LS and for each frame member and the system fragility curves are derived by a series arrangement of the component fragilities. Fig. 8a reports the component fragility curves for the case of the bare frame. Joint failure in tension resulted to be the most critical LS, however this LS provides only a measure of the damage of the joints due to the concrete degradation and it is not deemed as critical as the failure of the joint in compression. For this reason, it is disregarded in developing the system fragility curve. Concrete crushing in compression (LS1) is the most critical failure modality, steel rupture (LS2) is much less probable and failure of joints in compression and shear failure have a zero probability of occurrence.

Fig. 8b contains the fragility curve of the most vulnerable elements and of the system for three retrofit levels ( $\alpha=0.4, 1.6, 3.2$ ). The most vulnerable components of the bare frame are columns C1-2 and C1-3, failing in concrete crushing mode and exhibiting similar vulnerability. Fig. 8b shows that for  $\alpha=0.4$  the vulnerabilities of the two columns remain comparable, and are similar to the vulnerability of the most critical dissipative brace (D-1). This confirms the reliability of the simplified design procedure, which has the main aims of avoiding drastic changes to the internal action distribution in the frame and of achieving a simultaneous failure of the frame and the braces. In the case of  $\alpha=1.6$ , the fragility of the most critical frame component and of D-1 are very close, however column C1-2 is more vulnerable than C1-3. This is consequence of the higher level of axial load on column C1-2 with respect to C1-3 due to the bracing configuration. The results of the case of  $\alpha=3.2$  confirm this trend. As can be observed by Fig. 8b this phenomenon, which is not considered in the braces design procedure, induces a significant reduction of the retrofit effectiveness for high  $\alpha$  values.

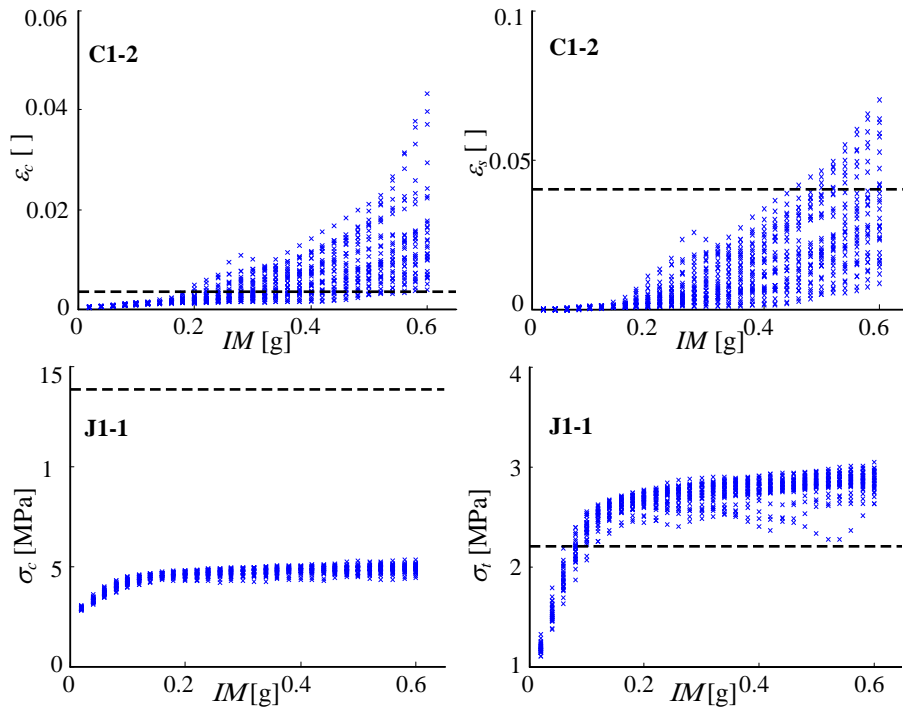


Figure 6. Demand samples and corresponding capacity limits for the case of bare frame.

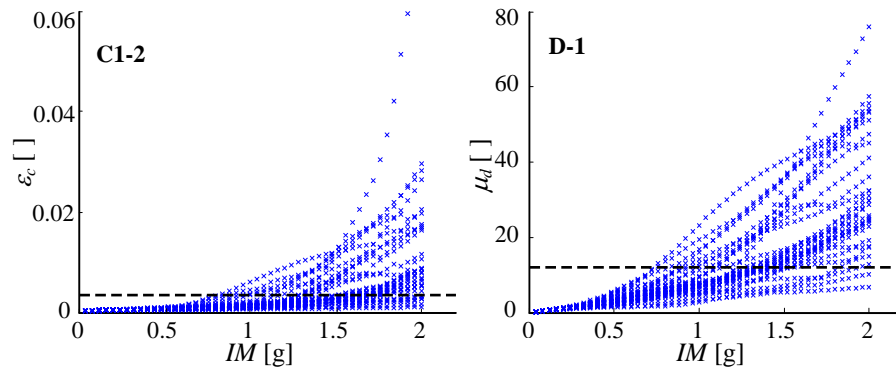


Figure 7. Demand samples and corresponding capacity limits for  $\alpha=1.6$ .

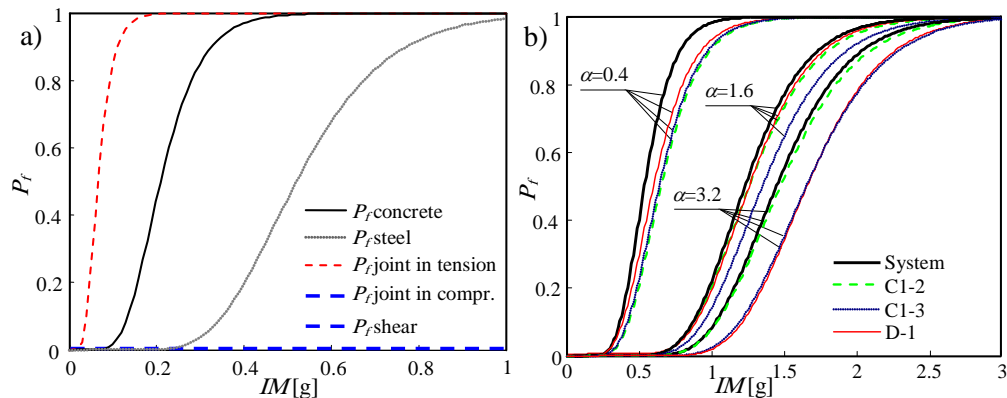


Figure 8. a) Lognormal fragility curves for the different failure modes and b) Fragility curve of the system and of the most vulnerable components for three retrofitted cases.

## 6. Conclusions

The paper illustrates a probabilistic methodology for assessing the vulnerability of RC buildings with limited ductility capacity retrofitted by means of dissipative braces and evaluating the behavior of the single resisting components. The methodology is based on the development of fragility curves of the bare and the retrofitted frames. It involves performing

IDA to account for the randomness of the earthquake excitation. Local EDPs are used to capture the modifications of the frame response induced by the introduction of the bracing system. Numerical fragility curves are derived by comparing the samples of the demand with the corresponding capacity limits and analytical fragility curves are defined by least-square minimization. The component fragility curves are built for each single structural component and for each single LS considered, while the system fragility curves are derived by assuming a series arrangement of the component LS. The capability of the proposed methodology is illustrated by considering a realistic benchmark RC frame retrofitted by BRBs. In this example is showed how the comparison of the single components fragility curves permits to individuate the most vulnerable elements of the frame that may change by increasing the retrofit level.

## 7. References

- [1] SOONG, T.T., SPENCER, B.F., “Supplemental energy dissipation: state-of-the-art and state-of-the-practice”, *Engineering Structures*, Vol. 24, No. 3, March 2002, pp. 243-259.
- [2] HUESTE, M.D., BAI, J.W., “Seismic Retrofit of a Reinforced Concrete Flat-Slab Structure: Part II - Seismic Fragility Analysis”, *Engineering Structures*, Vol. 29, No. 6, June 2007, pp. 1178-1188.
- [3] GUNEYISI, E.M., ALTAY, G., “Seismic fragility assessment of effectiveness of viscous dampers in R/C buildings under scenario earthquakes”, *Structural Safety*, Vol. 30, No. 5, September 2008, pp. 461-480.
- [4] GUNEYISI, E.M., “Seismic reliability of steel moment resisting framed buildings retrofitted with buckling restrained braces”, *Earthquake Engineering and Structural Dynamics*, Vol. 41, No. 5, April 2012, pp. 853-874.
- [5] LUPOI, G., LUPOI, A., PINTO, P.E., “Seismic risk assessment of rc structures with the “2000 SAC/FEMA” method”, *Journal of Earthquake Engineering*, Vol. 6, No. 4, 2002, pp. 499-512.
- [6] VAMVATSIKOS, D., CORNELL, C.A., “Incremental Dynamic Analysis”, *Earthquake Engineering and Structural Dynamics*, Vol. 31, No. 3, March 2002, pp. 491-514.
- [7] AYCARDI, L.E., MANDER, J.B., REINHORN, A.M., “Seismic resistance of reinforced concrete frame structures designed only for gravity loads: experimental performance of subassemblages”, *ACI Structural Journal*, Vol. 91, No. 5, September 1994, pp. 552-563.
- [8] BRACCI, J.M., REINHORN, A.M., MANDER, J.B., “Seismic resistance of reinforced concrete frame structures designed for gravity loads: performance of structural system”, *ACI Structural Journal*, Vol. 92, No. 5, September 1995, pp. 597-608.
- [9] MCKENNA, F., FENVES, G.L., SCOTT, M.H., “OpenSees: Open system for earthquake engineering simulation”, *Pacific Earthquake Engineering Center*, University of California, Berkeley, CA, 2006.
- [10] SCOTT, M.H., FENVES, G.L., “Plastic hinge integration methods for force-based beam-column elements”, *Journal of Structural Engineering*, Vol. 132, No. 2, February 2006, pp. 244-252.
- [11] PANAGIOTAKOS, T.B., FARDIS, M.N., “Deformation of reinforced concrete members at yielding and ultimate”, *ACI Structural Journal*, Vol. 98, No. 2, March 2001, pp. 135-148.
- [12] DALL’ASTA, A., TUBALDI, E., RAGNI, L., FREDDI, F., “Design methods for existing RC frames equipped with elasto-plastic or viscoelastic dissipative braces”, *Proceedings of XIII Convegno Nazionale ANIDIS*, Bologna, Italy, 2009.